

# Physical Properties of Polyurethane Plastic Sheets Produced from Polyols from Canola Oil

Xiaohua Kong and Suresh S. Narine\*

Alberta Lipid Utilization Program, Department of Agricultural Food and Nutritional Science,  
4-10 Agriculture/Forestry Centre, University of Alberta, Edmonton, Alberta T6G 2P5, Canada

Received January 5, 2007; Revised Manuscript Received March 1, 2007

Polyurethane (PUR) plastic sheets were prepared by reacting polyols synthesized from canola oil with aromatic diphenylmethane diisocyanate. The properties of the material were measured by dynamic mechanical analysis (DMA), differential scanning calorimetry (DSC), and thermogravimetric analysis (TGA) as well as tensile properties measurements. The effect of stoichiometric balance (i.e., OH/NCO molar ratio) on the final properties was evaluated. The concentration of elastically active network chains (EANCs),  $\nu_e$ , of the polymer networks was calculated using rubber elasticity theory. The glass transition temperatures ( $T_g$ ) for the plastic sheets with OH/NCO molar ratios of 1.0/1.0, 1.0/1.1, and 1.0/1.2 were found to be 23, 41, and 43 °C, respectively. The kinetic studies of the degradation process of the PUR plastics showed three well-defined steps of degradation. The PUR plastic sheets with OH/NCO molar ratio 1.0/1.1 had the highest  $\nu_e$ , lowest number-average molecule weight between cross-links,  $M_C$ , and excellent mechanical properties, indicating that this is the optimum ratio in the PUR formulations.

## Introduction

Polyurethanes (PURs) are one of the most interesting classes of copolymers, which can vary from rubbery materials to glassy thermoplastics and from linear polymers to thermosetting plastics.<sup>1</sup> The production of PUR is based on the reaction of organic isocyanates with compounds containing active hydroxyl groups such as polyols.<sup>2</sup> The investigation of structure–property relationships in PUR has gained great practical and theoretical importance, due to their various applications. As it is well-known,<sup>2</sup> many factors influence the physical, chemical, and thermal properties of PUR. These include the volume fractions of the soft and hard segments, the chemical compositions of these segments and distribution of each segment, and the degree of cross-linking. These factors could be manipulated by varying the stoichiometric balance of the components in the reaction (polyol/isocyanate or OH/NCO ratio).

PUR are traditionally industrially produced by reacting petroleum-based polyols with isocyanates. With the realization that oil resources are becoming increasingly hard to find and expensive to produce, researchers have sought different ways and technologies to viably produce plastics from renewable resources.<sup>3–12</sup> As an inexpensive, readily available candidate, attention has been paid to vegetable oils which are abundant and varied as a source for polymeric materials. To produce valuable polymeric materials from vegetable oils, functional groups such as hydroxyl, epoxy, or carboxyl groups have to be introduced to the fatty acid chains of the vegetable oils.<sup>3–13</sup> Höfer and co-workers, for example, have produced polyols and polymers from renewable resources that are successfully commercialized.<sup>5,7,12</sup>

Our research effort is part of the growing worldwide interest in the development of vegetable-oil-based polyurethanes. Ozonolysis technology has been industrially established and has been used to produce azelaic acid and pelargonic acid from com-

mercial-grade oleic acid.<sup>14</sup> Generally, the process of producing acids is carried out in carboxylic acid. To produce alcohols using this technology, the conversion of the ozonide to acids during ozonolysis should first be prevented. In our case, this has been achieved to great extent by using a nonacid solvent. The products of such ozonolysis (the ozonide) have been further reduced to aldehyde using a reductive agent and subsequently hydrogenated to produce the alcohols.

We have used this ozonolysis- and hydrogenation-based technology to produce polyols with terminal hydroxyl groups from vegetable oils<sup>15–17</sup> and used them successfully to produce PUR elastomers and foams which had better thermomechanical and mechanical properties than the corresponding PUR made from commercially available biobased polyols.<sup>15,16</sup> This first generation of polyols was not suitable to produce PUR plastics due to their relatively high acidity content. Recently, we have improved the technology and optimized the process and produced a new generation of polyols from canola oil with lower acidity and hydroxyl number close to what is theoretically achievable. The polyols were suitable for the production of a wider range of PUR materials including PUR plastics.

In this paper, we report on the properties of PUR plastic sheets prepared using the new generation of polyols synthesized from canola oil. The stoichiometric balance (i.e., OH/NCO molar ratio), a particularly important parameter, was used to control the final properties of the material. The physical and thermal properties were studied using dynamic mechanical analysis (DMA), differential scanning calorimetry (DSC), and thermogravimetric analysis (TGA) techniques. The concentration of elastically active network chains (EANCs),  $\nu_e$ , of the polymer networks was calculated using rubber elasticity theory. The effects of OH/NCO molar ratio on the properties of PUR are also discussed.

## Experimental Section

**Materials.** The canola vegetable oil used in this study was a “100% Pure Canola” supplied by Canbra Foods Limited, Lethbridge, AB,

\* To whom correspondence should be addressed. Phone: 1-780-492-9081. Fax: 1-780-492-7174. E-mail: Suresh.narine@ualberta.ca.

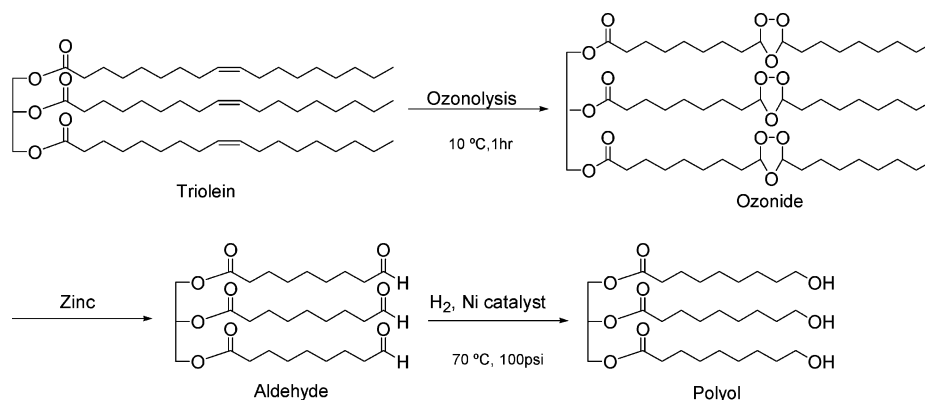


**Figure 1.** Reaction scheme of polyol using triolein as an example. The individual curves are labeled (a) PUR plastic sheets with OH/NCO molar ratio 1.0/1.0, (b) PUR plastic sheets with OH/NCO molar ratio 1.0/1.1, and (c) PUR plastic sheets with OH/NCO molar ratio 1.0/1.2.

Canada. Raney nickel 2800 (slurry in water) catalyst was obtained from Sigma-Aldrich Co., Milwaukee, WI. Ethyl acetate (reagent grade) and zinc (30 meshes, granular) were obtained from Fisher Scientific. The aromatic diphenylmethane diisocyanate (MDI, Mondur MRS) was sourced from Bayer Corp., Pittsburgh, PA. NCO content of MDI was 31.5 wt %, and its functionality was 2.6 as provided by the supplier.

**Synthesis of Polyol.** Canola-oil-based polyol has been synthesized using ozonolysis- and hydrogenation-based technology. Canola oil in the ethyl acetate (volume of 1:4) was ozonized (20% volume solution) at 10 °C and 5 L/min O<sub>2</sub> flow rate (with the concentration of ozone of 62 g/m<sup>3</sup>) for 1 h. The ozonolysis product was reduced by zinc (molar ratio of 1:1.2 of equivalent weight) at room temperature, followed by hydrogenation at 70 °C and with 100 psi with Raney nickel as catalyst. Finally, the solvent was removed by rotary evaporation and the low molecular byproducts were removed by wiped blade molecular distillation. The reaction scheme is illustrated in Figure 1 using triolein as an example. Due to the nature of the starting materials, the obtained material was a typical polyester polyol.

**Preparation of the Plastics.** The PUR plastic sheets were prepared by reacting the polyols with aromatic diphenylmethane diisocyanate. Three different molar ratios of the OH group to the isocyanate (NCO) group ( $M_{\text{ratio}}$ ), i.e. OH/NCO of 1.0/1.0, 1.0/1.1, and 1.0/1.2, were chosen for the formulations. The desired OH/NCO molar ratio satisfies the following equation:

$$M_{\text{ratio}} = \frac{W_{\text{polyol}}/EW_{\text{polyol}}}{(W_{\text{PU}} - W_{\text{polyol}})/EW_{\text{isocyanate}}} \quad (1)$$

Here  $W_{\text{polyol}}$  is the weight of the polyol,  $EW_{\text{polyol}}$  is the equivalent weight of polyol,  $W_{\text{PU}}$  is the total weight of PUR to produce, and  $EW_{\text{isocyanate}}$  is the equivalent weight of the isocyanate.

The equivalent weight for the isocyanate was provided by the supplier and is  $EW_{\text{isocyanate}} = 133$  g/mol. The equivalent weights of polyol were determined using the following equation:

$$EW_{\text{polyol}} = \frac{\text{molecular weight of KOH} \times 1000}{\text{OH no.}} = \frac{56110}{\text{OH no.}} \text{ g/mol of hydroxyl groups}$$

The weight of the polyol and isocyanate were calculated using the above calculated equivalent weight.

Suitable amounts of polyol and MDI were weighed in a plastic container and stirred slowly for 2 min. The mixture was cast directly into a metallic mold previously greased with silicone release agent and placed in an oven at 60 °C for polymerization. The samples were postcured at 60 °C for 48 h. The plastic sheets were 100 × 100 × 2 mm, ready for further characterization.

**Rheometric Measurements.** Viscosity of the polyol was measured in shearing mode with the TA Advanced Rheometer AR 2000 using a constant shearing rate of 51.6 s<sup>-1</sup>.

**Density Tests.** The density of the PUR plastic sheets with different molar ratio was determined according to ASTM D 792-00 standard.

**FTIR.** The FTIR spectra were recorded on a Nicolet Magna 750 FTIR, equipped with an MCT-A detector and a Nicolet Nic-Plan IR microscope used in transmission mode. The spectra were recorded in the range 650–4000 cm<sup>-1</sup> with a nominal resolution of 4 cm<sup>-1</sup>. A background spectrum was first collected before each absorbance spectrum. A total of 128 interferograms were coadded before Fourier transformation using the Nicolet Omnic software.

**Thermal Properties.** DSC measurements were carried out on a DSC Q100 (TA Instruments), equipped with a refrigerated cooling system. All the DSC measurements were performed following the ASTM E1356-03 standard procedure. The samples were heated at a rate of 10 °C/min from 25 to 80 °C to erase thermal history, cooled to -40 °C at a cooling rate of 5 °C/min, and then heated again to 80 °C at a heating rate of 10 °C/min. The second heating stage was selected to be analyzed for the collection of melting data. All the procedures were performed under a dry nitrogen gas atmosphere.

DMA measurements were carried out on a DMA Q800 (TA Instruments) equipped with a liquid-nitrogen cooling apparatus in the single cantilever mode, with a constant heating rate of 1 °C/min from -120 to 80 °C. The size of the samples was 18 × 7 × 2 mm. The measurements were performed following ASTM E1640-99 standard at a fixed frequency of 1 Hz and a fixed oscillation displacement of 0.015 mm. In the case of multiple isothermal oscillation experiments, the isothermal evolution of rheological parameters was recorded as a function of frequency ranging from 0.1 to 100 Hz. The measurements were performed, every 5 °C, 30 °C below and above glass transition temperature.

TGA was carried out on a TGA Q50 (TA Instruments) following the ASTM D3850-94 standard. The sample was ground to a powder after chilling with liquid nitrogen, and approximately 20 mg of the specimen was loaded in the open platinum pan. The samples were heated from 25 to 600 °C under dry nitrogen at constant heating rates of 2.5, 5, 10, 15, and 20 °C/min.

All the samples were run in triplicate for thermal property measurements. The reported errors are the subsequent standard deviations.

**Mechanical Properties.** Specimens for tensile measurements were cut out from the PUR plastic sheets using an ASTM D638 type V cutter. The tests were performed at room temperature using an Instron (MA) tensile testing machine (model 4202) equipped with a 500 Kg load cell and activated grips which prevented slippage of the sample before break. The used cross-head speed was 100 mm/min, as suggested by the above-mentioned ASTM standard. At least five identical dumbbell-shaped specimens for each sample were tested, and their average mechanical properties are reported. The reported errors are the subsequent standard deviations.

**Table 1.** Polyols and Diisocyanate Parameters Used in the Formulations To Prepare the PUR Plastic Sheets<sup>a</sup>

	equiv wt	OH no.	acidity no.	viscosity at 25 °C
type	(g/mol)	(mg of KOH/g)	(mg of KOH/g)	(Pas)
polyol	239	235 ± 5	16 ± 2	0.9860 ± 0.0005
MDI	133			

<sup>a</sup> Errors are standard deviations; *n* = 3.

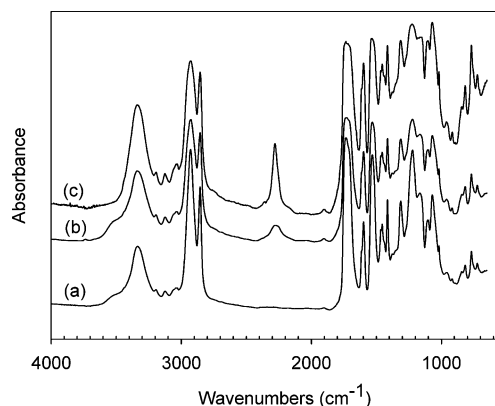
## Results and Discussion

The hydroxyl and acidity values of the polyol were determined according to ASTM titration methods D1957-86 and ASTM D4662-98, respectively. The average values and standard deviations of triplicate measurements are reported in Table 1. As listed in Table 1, the hydroxyl number (235 mg of KOH/g) is close to the maximum value of 251 mg of KOH/g theoretically obtainable when producing polyol by assuming that all the double bonds are cleaved.<sup>18</sup> The use of a mild solvent (ethyl acetate) and zinc reduction procedure has greatly improved the ozonolysis- and hydrogenation-based technology and yielded a polyol with higher hydroxyl value and lower acidity content than that of the polyol previously made. The composition of the polyol was determined by an analysis protocol developed in our laboratory on the basis of the HPLC procedure developed by Elfman-Borjesson and Harrod<sup>19</sup> for the analysis of lipid derivatives. The polyol contained about 60%, 26%, and 5% (on a mass basis) of triol, diol, and monoal, respectively. The remaining were saturated triacylglycerols (TAGs). The production of monoal and diol is unavoidable since the starting oil contains TAGs (20.6%)<sup>18</sup> that have a mixture of saturated fatty acids (which cannot be functionalized) and unsaturated fatty acids. Monoal and diol can also be produced if the ozonolysis reaction does not cleave all the double bonds on all the fatty acid chains.

Due to oxidation, either during or after ozonolysis, part of the ozonide was oxidized to carboxylic acid which could not be hydrogenated.<sup>20</sup> The polyol ended up with relatively high acid number (16 ± 2 mg of KOH/g). Despite the relatively high acid content, the polyol was still capable of producing PUR plastics, as long as a relatively higher isocyanate content was used in the formulation to compensate for the detrimental effect of the acid. Note that one can minimize further the acids content by taking the following precautions: (1) dry the solvent (here the ethyl acetate) by using for example molecular sieve to get rid of the moisture; (2) perform ozonolysis reaction at lower temperature.

The FTIR spectra of the three PUR plastics with different OH/NCO molar ratios are shown in Figure 2. A strong 3340 cm<sup>-1</sup> absorbance band characteristic of the N—H group and an absorbance band characteristic of the C=O group centered around 1700 cm<sup>-1</sup> are present in all the FTIR spectra demonstrating the formation of urethane linkages in all the samples. As shown in Figure 2, the intensities of the N—H group absorption band increase with decreasing OH/NCO molar ratio. This evidenced that the concentration of the urethane linkages in the PUR plastics with OH/NCO molar ratio 1.0/1.2 is much higher than those of the other two formulations. Furthermore, the —NCO group absorption band centered at 2270 cm<sup>-1</sup> is clearly missing in the case of OH/NCO molar ratio 1.0/1.0, while it increases significantly with decreasing OH/NCO molar ratio, indicating that PUR plastics with OH/NCO molar ratio 1.0/1.2 contained more unreacted —NCO groups than the other two.

FTIR spectroscopy gives useful qualitative information about the molecular structure of the PUR, but to obtain quantitative

**Figure 2.** FTIR spectra of the PUR plastic sheets. The individual curves are labeled (a) PUR plastic sheets with OH/NCO molar ratio 1.0/1.0, (b) PUR plastic sheets with OH/NCO molar ratio 1.0/1.1, and (c) PUR plastic sheets with OH/NCO molar ratio 1.0/1.2.

information, other methods, such as DMA which could be used to determine the concentration of EANCs in the network, are needed.

The elastic behavior of polymer networks can be described by either the affine or the phantom network models.

In the affine network model,<sup>21</sup> the storage shear modulus  $G'$  is given by

$$G' = \frac{E'}{3} = \nu_e RT = \frac{\rho RT}{M_c} \quad (2)$$

where  $R$  is the gas constant,  $\nu_e$  the concentration of EANCs,  $T$  the absolute temperature,  $M_c$  the number-average molecular weight between cross-links, and  $\rho$  the density of the PUR plastic sheets.

The phantom network model,<sup>22</sup> which usually describes the elasticity of perfect networks, considers the effect of elastically active junctions. However, in real PURs, most of the networks have less than perfect elasticity. For example, nonidealities such as dangling chains will decrease  $\nu_e$  and entrapped entanglements will increase it. The molecular chains will also interact with each other and reduce the junction fluctuations.

In the case of strong interactions, the junctions do not fluctuate at all and are displaced affinely with macroscopic strain.<sup>23</sup> Because of the strong interactions between molecular chains in the PUR network, the storage shear modulus  $G'$  of the PUR network could be related to  $\nu_e$  using the affine network model (eq 2). Using the time-temperature superposition principle,<sup>24</sup> it is possible to characterize the viscoelastic behavior of a polymer at various temperatures over an experimental unapproachable time or temperature range.

Isothermal oscillation measurements were performed in the  $T_g$  region. The isothermal storage moduli ( $E'$ ) were obtained as a function of frequency. The curves obtained at different temperatures were superposed in the standard manner into respective master curves using the time-temperature superposition principle. Figure 3 shows the master curve of  $E'$  at a reference temperature of  $T_g + 5$  °C for PUR plastic sheet with OH/NCO molar ratio 1.0/1.2. The extended frequency range obtained by the superposition is 10<sup>-5</sup>–10<sup>9</sup> Hz. The pseudoequilibrium modulus of the cross-linking network,  $G'$  ( $G' = E'/3$ ), is related to  $\nu_e$  through eq 2.  $\rho$  was determined according to ASTM D 792-00 standard and assumed to be a constant when the  $M_c$  was calculated at temperature of  $T_g + 5$  °C. The results are listed in Table 2.

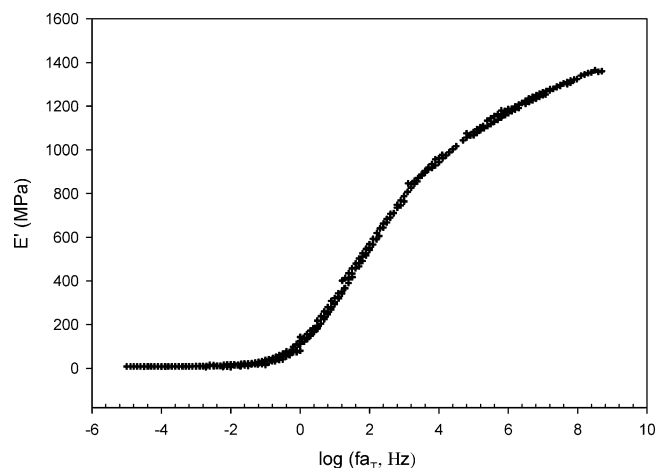


**Figure 3.** Master curve of  $E'$  at a reference temperature of  $T_g + 5$  °C for PUR plastic sheet with OH/NCO molar ratio 1.0/1.2.

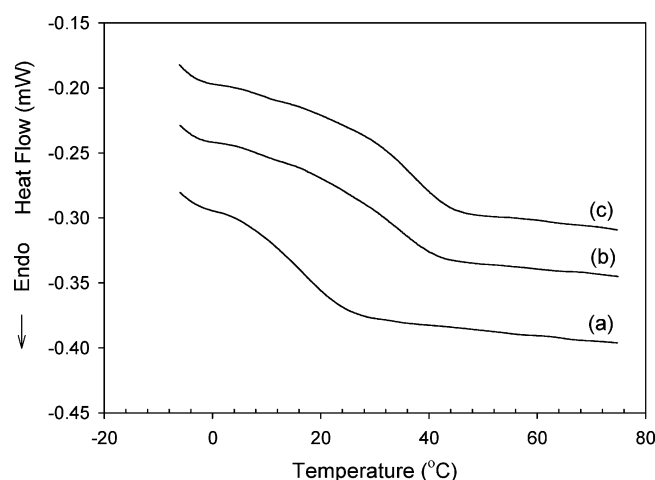


**Figure 4.** MDSC curves of the PUR plastic sheets. The individual curves are labeled (a) PUR plastic sheets with OH/NCO molar ratio 1.0/1.0, (b) PUR plastic sheets with OH/NCO molar ratio 1.0/1.1, and (c) PUR plastic sheets with OH/NCO molar ratio 1.0/1.2.

The PUR plastic sheets with  $M_{ratio} = 1.0/1.1$  has the highest  $\nu_e$  and lowest  $M_C$ . For  $M_{ratio} = 1.0/1.0$  and  $M_{ratio} = 1.0/1.2$ ,  $\nu_e$  and  $M_C$  of the plastic sheets remained almost the same. This indicated that only reasonable excess of isocyanates can improve the network structure by increasing the concentration of EANCs in the network. Too much off-stoichiometry resulted in incomplete conversion of isocyanates, which is the main reason for the formation of imperfect structures and the decrease of the concentration of EANCs in the networks.<sup>25,26</sup>

$T_g$  was investigated using both DSC and DMA. The DSC curves of the PUR plastic sheets with different molar ratios, shown in Figure 4, display a single feature: a glass transition in the range 20–45 °C.  $T_g$  was determined from the shift of heat capacity with temperature. Figures 5 and 6 show the changes in the storage ( $E'$ ) and loss ( $E''$ ) moduli of the PUR plastic sheets with temperature, obtained from DMA carried out at frequency of 1 Hz, respectively.  $T_g$  values as determined from the inflection point of  $E'$  vs temperature are higher than

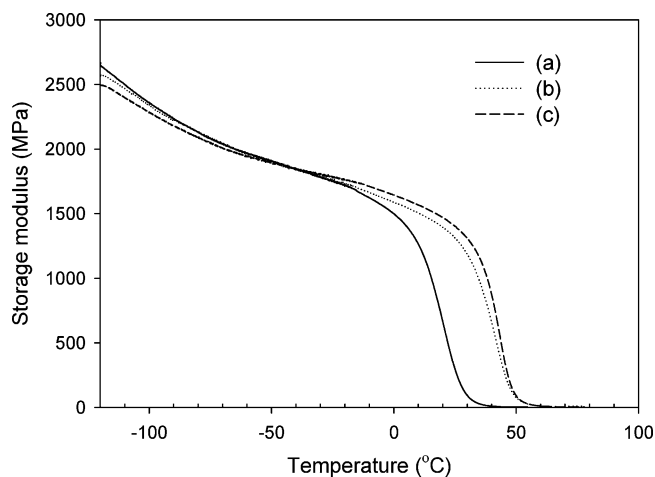


**Figure 5.** Storage moduli vs temperature, obtained from DMA carried out at a frequency of 1 Hz. The individual curves are labeled (a) PUR plastic sheets with OH/NCO molar ratio 1.0/1.0, (b) PUR plastic sheets with OH/NCO molar ratio 1.0/1.1, and (c) PUR plastic sheets with OH/NCO molar ratio 1.0/1.2.

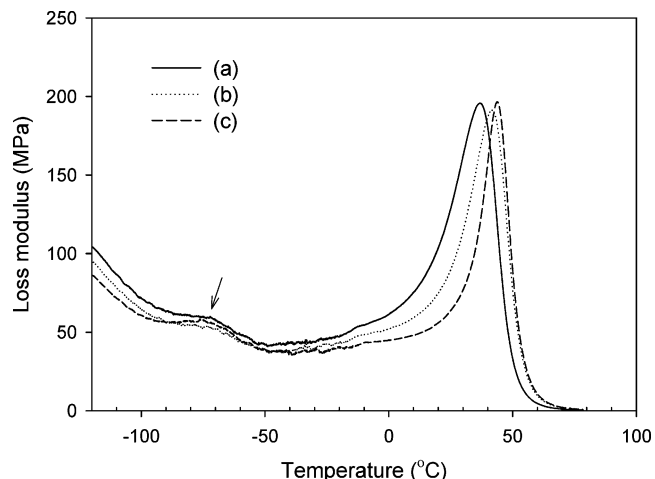


**Figure 6.** Changes in the loss ( $E''$ ) moduli with temperature, obtained from DMA carried out at frequency of 1 Hz. The individual curves are labeled (a) PUR plastic sheets with OH/NCO molar ratio 1.0/1.0, (b) PUR plastic sheets with OH/NCO molar ratio 1.0/1.1, and (c) PUR plastic sheets with OH/NCO molar ratio 1.0/1.2.

those determined by DSC by about 5–10 °C (see Table 2) as generally found in the literature.<sup>9</sup> The trend is however the same: the lowest  $T_g$  was recorded for the PUR plastic sheet with the OH/NCO molar ratio 1.0/1.0 and the highest  $T_g$  was recorded for the PUR plastic sheet with the OH/NCO molar ratio 1.0/1.2. The  $T_g$  value for the OH/NCO molar ratio 1.0/1.1 sample is close to that of the OH/NCO molar ratio 1.0/1.2 sample.

The glass transition of a polymer network is affected by the concentration of EANCs as well as the chemical structure. In principle, increased aromatic content should result in higher  $T_g$ , and reduced  $\nu_e$  would affect it oppositely.<sup>10</sup> The relatively large increase of  $T_g$  (~20 °C) when  $M_{ratio}$  decreased from 1.0/1.0 to 1.0/1.1 indicated that the flexibility of the polymer chains was

**Table 2.**  $T_g$  (°C) Obtained by DSC and DMA, Density, and Parameters of Cross-Linking Networks of the PUR Plastic Sheets

molar ratio (OH/NCO)	$T_g$ (°C) from DSC	$T_g$ (°C) from DMA	$E'$ (MPa) <sup>a</sup>	$\rho$ at 23 °C (g/cm <sup>3</sup> )	$\nu_e$ (mol/cm <sup>3</sup> )	$M_C$ (g/mol)
1.0/1.0	15.3 ± 0.6	22.7 ± 0.6	5.1	1.133	6.8 × 10 <sup>-4</sup>	1662
1.0/1.1	34.3 ± 0.6	41.3 ± 0.6	8.3	1.145	1.0 × 10 <sup>-3</sup>	1217
1.0/1.2	36.7 ± 0.6	43.0 ± 1.0	6.1	1.156	7.6 × 10 <sup>-4</sup>	1682

<sup>a</sup>  $E'$  at rubbery plateau from master curve.



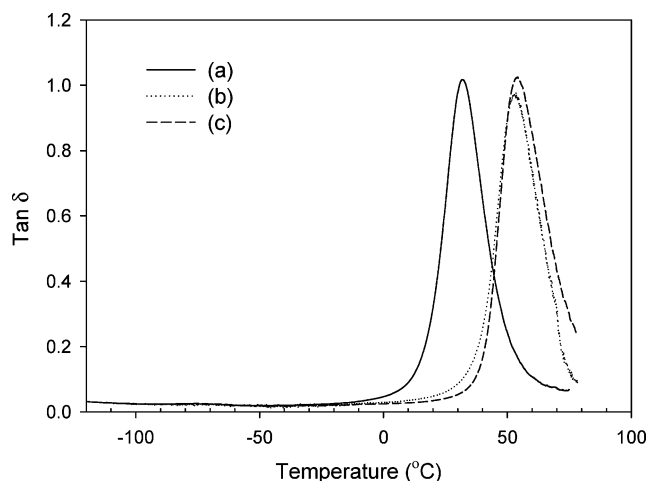


**Figure 7.** Temperature dependence of tangent  $\delta$  ( $\tan \delta$ ) measured by DMA for the PUR plastic sheets. The individual curves are labeled (a) PUR plastic sheets with OH/NCO molar ratio 1.0/1.0, (b) PUR plastic sheets with OH/NCO molar ratio 1.0/1.1, and (c) PUR plastic sheets with OH/NCO molar ratio 1.0/1.2.

reduced for the higher cross-linked networks, shifting the rubbery state to higher temperatures. This could be explained by the high value of  $\nu_e$  for the sample with  $M_{\text{ratio}}$  of 1.0/1.1 as mentioned earlier. However, when the OH/NCO molar ratio further decreased from 1.0/1.1 to 1.0/1.2,  $T_g$  remained almost the same. This is thought to be due to several competing factors including primarily: (1) lower  $\nu_e$  of the PUR plastic sheets with OH/NCO molar ratio 1.0/1.2; (2) increased phenyl-ring content produced by larger amount of isocyanate in the later formulation.

A weak transition at about  $-70^\circ\text{C}$  was also observed for all our samples as illustrated by the first peak in the loss moduli curves (arrow 1 in Figure 6). This transition which has been detected in PUR produced from other vegetable oils<sup>13</sup> has been identified as the  $\beta$  transition. The  $\beta$  transition may be related to the movements of a chain part containing the urethane group attached to cross-linker<sup>27</sup> or to the motion of the backbone chain of the short groups in the fatty acid chains.<sup>28</sup>

The height and width of  $\tan \delta$  peaks may also be analyzed for each PUR plastic sheet to observe trends in the concentration of EANCs and network homogeneity.<sup>29,30</sup> As shown in Figure 7, the height of the  $\tan \delta$  peak measured by DMA is the lowest (0.98) for OH/NCO molar ratio 1.0/1.1 and has approximately the same value for the two other formulations (1.02 for OH/NCO molar ratio 1.0/1.0 and 1.03 for OH/NCO molar ratio 1.0/1.2). The full width at half-maximum of  $\tan \delta$  peak is 19, 21, and 22  $^\circ\text{C}$  for samples with OH/NCO molar ratio 1.0/1.0, 1.0/1.1 and 1.0/1.2, respectively. Because  $\tan \delta$  is the ratio of viscous to elastic components of the modulus, it can be speculated that its decreasing height is related to lower segmental mobility and thus indicative of a higher  $\nu_e$ . The evolution of  $\tan \delta$  peak height with OH/NCO molar ratio reflects that of  $\nu_e$  and demonstrates consistency with what has been discussed in light of the theory of rubber elasticity. On the other hand, the slight broadening of the  $\tan \delta$  peak with decreasing OH/NCO molar ratio is probably due to the excess of isocyanate which may have reacted with the amine (produced by the side reactions of the isocyanate with moisture or carboxylic acids) to form urea. The formation of urea linkages increases the number of cross-linking joints and results in a wider distribution of network structures.

TGA curves of the PUR plastic sheets with different OH/NCO molar ratios at  $5^\circ\text{C}/\text{min}$  heating rate and their derivatives (DTGA) are shown in Figure 8a,b, respectively. For all the

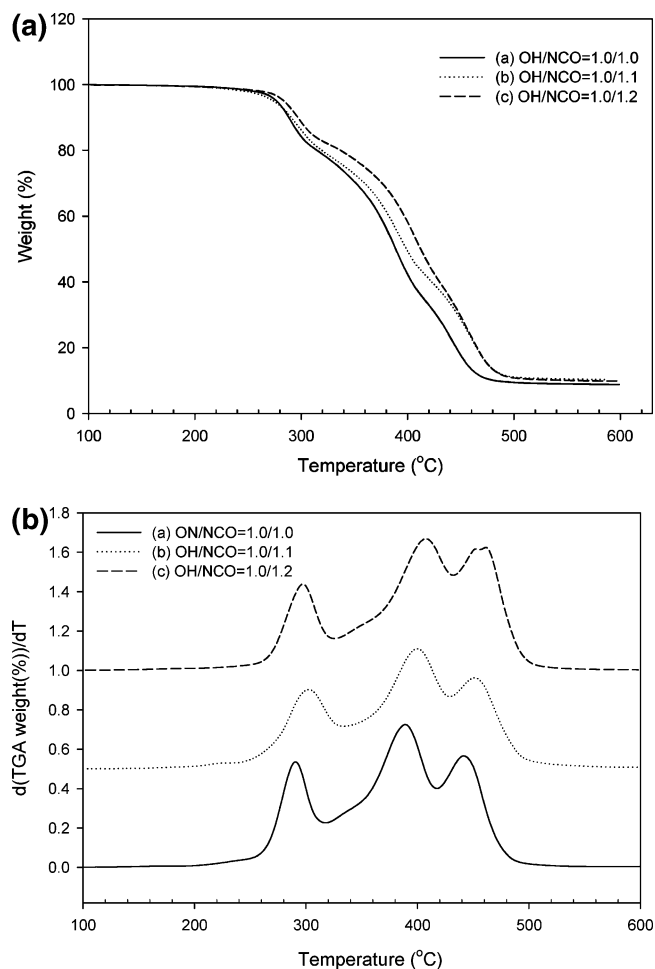


**Figure 8.** (a) TGA curves of the PUR plastic sheets at  $5^\circ\text{C}/\text{min}$  heating rate. (b) TGA derivative (DTGA) curves of the PUR plastic sheets at  $5^\circ\text{C}/\text{min}$  heating rate. The individual curves are labeled (a) PUR plastic sheets with OH/NCO molar ratio 1.0/1.0, (b) PUR plastic sheets with OH/NCO molar ratio 1.0/1.1, and (c) PUR plastic sheets with OH/NCO molar ratio 1.0/1.2.

formulations, the decomposition started at approximately  $200^\circ\text{C}$  and ended at  $500^\circ\text{C}$ . The shapes of the weight loss curves were similar in the whole temperature range. DTGA curves revealed three main degradation processes. In the first step the sample lost 20% of its weight, in the second step it lost 20–70%, and in the third it lost its remaining weight.

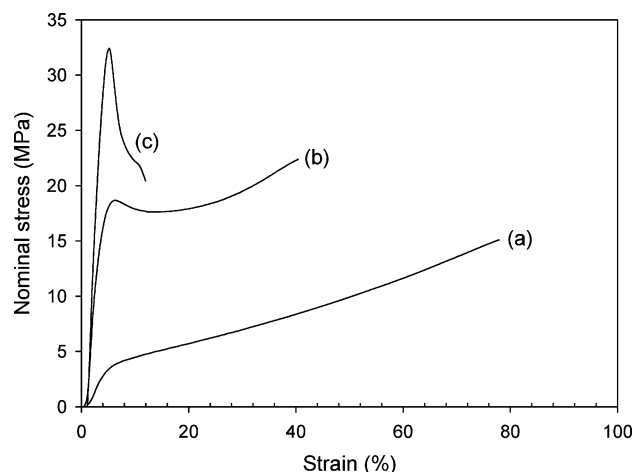
Kinetic studies of the degradation process were performed to better understand the thermal degradation behavior of the PUR plastic sheets. The kinetic data for thermal degradation, namely, the activation energy  $E$ , depends on heating rate.<sup>31</sup> Because the kinetics of degradation is so complex, different methods applied to real polymers give substantially different results.<sup>32</sup> The values obtained for the activation energy depend significantly on the mathematical treatment used for the calculations as well.<sup>33</sup>

In this study, the Kissinger method<sup>34</sup> based on multiple heating rates was applied to analyze TGA kinetic data. This method involves the temperature values,  $T_m$ , at the maxima of the first derivative weight loss of the DTGA curves. Kissinger assumed that pseudo-first-order kinetics for the thermal decomposition could be used such that the following expression could be derived:

$$\frac{d[\ln(\beta/T_m^2)]}{d(1/T_m)} = \frac{-E}{R} \quad (3)$$

**Table 3.** Activation Energies Calculated by Kissinger's Method

OH/NCO	step I		step II		step III	
	$\alpha$ range	$E$ (kJ/mol)	$\alpha$ range	$E$ (kJ/mol)	$\alpha$ range	$E$ (kJ/mol)
1.0/1.0	0.1–0.2	120	0.2–0.7	180	0.7–0.9	220
1.0/1.1	0.1–0.2	140	0.4–0.7	140	0.7–0.9	270
1.0/1.2	0.1–0.2	110	0.2–0.7	150	0.7–0.9	220

**Figure 9.** Nominal stress vs strain curves for the PUR plastic sheets. The individual curves are labeled (a) PUR plastic sheets with OH/NCO molar ratio 1.0/1.0, (b) PUR plastic sheets with OH/NCO molar ratio 1.0/1.1, and (c) PUR plastic sheets with OH/NCO molar ratio 1.0/1.2.

Here  $\beta$  is the heating rate,  $R$  the gas constant, and  $E$  the activation energy. Thus, a plot of  $\ln(\beta/T_m^2)$  vs  $1/T_m$  allows one to calculate the activation energies for the main stages of decomposition. The values of activation energy obtained using five different rates (2.5, 5, 10, 15, and 20 °C/min) are listed in Table 3.

As indicated by the Kissinger method, all the PUR plastic sheets decomposed in multiple stages. The first stage ( $\alpha < 0.2$ ) which is associated with  $E$  values in the range of 110–140 kJ/mol can be assigned to the cleavage of the urethane linkages.<sup>32</sup> The calculated activation energies for the intermediate stage ( $\alpha = 0.2–0.7$ ) is in the range 140–180 kJ/mol. In the last decomposition stage ( $\alpha = 0.7–0.9$ ), the  $E$  values calculated are fairly high (approximately 270 kJ/mol) close to the C–C bond dissociation energy of 348 kJ/mol suggesting a probable C–C bond cleavage.<sup>35</sup> The wide variation of  $E$  with  $\alpha$  is expected to be due to the continuous change of the degradation mechanism, suggesting the complexity of the thermal degradation of these polymers. This implies that  $E$  is not only a function of chemical structure of polymers but also changes with conversion for a single polymer. It provides, however, an additional parameter for the assessment of the thermal stability of these polymers.

The stress vs strain curves for the PUR plastic sheets with different OH/NCO molar ratios are shown in Figure 9. In the case of PUR plastic sheet with OH/NCO molar ratio 1.0/1.0, the tensile strength at break is  $14 \pm 2$  MPa and maximum elongation is  $75 \pm 10\%$ . PUR plastic sheet with OH/NCO molar ratio 1.0/1.1 displays a yield point with yield strength  $18 \pm 1$  MPa followed by a slight decrease and then increase until break at elongation of  $39 \pm 3\%$ . The PUR plastic sheet with OH/NCO molar ratio 1.0/1.2 is more rigid but brittle with tensile strength at yield  $32 \pm 2$  MPa and elongation at break of  $8 \pm 1\%$ . Again this is probably due to the excess of aromatic content in this series as mentioned before. Since  $T_g$  (23 °C) of the PUR

plastic sheet with OH/NCO molar ratio 1.0/1.0 coincides with the measuring temperature (25 °C), this polymer behaved as a hard rubber. If this product have been measured at a temperature significantly below it is  $T_g$ , it would have typical mechanical properties<sup>36</sup> of rigid plastics as the other two types of plastic sheets with  $T_g$  around 40 °C.

It is worth mentioning that ozonolysis as a low-cost and easily run technology, combined with the utilization of cheap and mild solvent, provides a great opportunity to industrially commercialize vegetable-oil-based polyol. It is reasonable to believe that the vegetable-oil-based PUR could be a potential candidate to replace or partially replace petroleum-based PUR, in sensitive and high end applications such as in the biomedical area. To this end, our group is currently engaged in further studies of PUR made from vegetable-oil-based polyols investigating their various properties and functionalities and comparing them with those of petroleum-based PUR.

## Conclusions

Polyurethane plastic sheets have been prepared by reacting polyols with terminal primary functional groups synthesized from canola oil with aromatic diphenylmethane diisocyanate. The  $T_g$  of the plastic sheets increased as the OH/NCO molar ratio was decreased. Three well-defined steps of degradation of the PUR plastics were observed by TGA, and the degradation process was analyzed using a model-free kinetic approach (Kissinger model). The properties of PUR plastic sheets were mainly governed by the stoichiometric balance of the components in the reaction and the degree of cross-linking. The PUR plastic sheets with OH/NCO molar ratio 1.0/1.1 had the highest  $\nu_e$ , lowest number-average molecule weight between cross-links  $M_c$ , and excellent mechanical properties, indicating that this is the optimum ratio in the PUR plastics formulation.

**Acknowledgment.** We acknowledge the technical contributions of Mr. Ereddad Kharraz. The financial support of Bunge Oils, AVAC Ltd., Alberta Agricultural Research Institute, Alberta Canola Producers Commission, Alberta Crop Industry Development Fund, Alberta Agriculture Food and Rural Development and NSERC is gratefully acknowledged.

## References and Notes

- Hepburn, C. *Polyurethane Elastomers*; Applied Science Publishers: New York, 1982; Chapter 2.
- Szycher, M. *Szycher's Handbook of Polyurethanes*; CRC Press: Boca Raton, FL, 1999.
- Khoe, T. H.; Otey, F. H.; Frankel, E. N. Rigid urethane foams from hydroxymethylated linseed oil and polyol esters. *J. Am. Oil Chem. Soc.* **1972**, 49 (11), 615–618.
- Lyon, C. K.; Garrett, V. H.; Frankel, E. N. Rigid urethane foams from hydroxymethylated castor oil, safflower oil, oleic safflower oil, and polyol esters of castor acids. *J. Am. Oil Chem. Soc.* **1974**, 51 (8), 331–334.
- Gruber, B.; Höfer, R.; Kluth, H.; Meffert, A. Polyole auf Basis fettchemischer Rohstoffe. *Fett. Wiss. Technol., Fat. Sci. Technol.* **1987**, 89 (4), 147–151.
- Barrett, L. W.; Sperling, L. H.; Murphy, C. J. Naturally functionalized triglyceride oils in interpenetrating polymer networks. *J. Am. Oil Chem. Soc.* **1993**, 70 (5), 523–534.

- (7) Heidbreder, A.; Höfer, R.; Grützmacher, R.; Westfechtel, A.; Blewett, C. W. Oleochemical products as building blocks for polymers. *Fett/Lipid* **1999**, *101* (11), 418–424.
- (8) Li, F.; Hanson, M. V.; Larock, R. C. Soybean oil-divinylbenzene thermosetting polymers: synthesis, structure, properties and their relationships. *Polymer* **2001**, *42* (4), 1567–1579.
- (9) Guo, A.; Demydov, D.; Zhang, W.; Petrovic, Z. S. Polyols and polyurethanes from hydroformylation of soybean oil. *J. Polym. Environ.* **2002**, *10* (1–2), 49–52.
- (10) Petrovic, Z. S.; Cevallos, M. J.; Javni, I.; Schaefer, D. W.; Justice, R. Soy-oil-based segmented polyurethanes. *J. Polym. Sci., Part B: Polym. Phys.* **2005**, *43* (22), 3178–3190.
- (11) Petrovic, Z. S.; Zhang, W.; Javni, I. Structure and properties of polyurethanes prepared from triglyceride polyols by ozonolysis. *Biomacromolecules* **2005**, *6* (2), 713–719.
- (12) Roloff, T.; Erkens, U.; Höfer, R. Polyols based on renewable feedstocks: A significant alternative. *Urethanes Technol.* **2005**, *22* (4), 29–33.
- (13) Zlatanovic, A.; Petrovic, Z. S.; Dusek, K. Structure and properties of triolein-based polyurethane networks. *Biomacromolecules* **2002**, *3* (5), 1048–1056.
- (14) Goebel, C. G.; Brown, A. C.; Oehlschlaeger, H. F.; Rolfes, R. P. U.S. Patent 2,813,113, 1957.
- (15) Narine, S. S.; Kong, X.; Bouzidi, L.; Sporns, P. Physical properties of polyurethanes produced from polyols from seed oils. II-foams. *J. Am. Oil Chem. Soc.* **2007**, *84*, 65–72.
- (16) Narine, S. S.; Kong, X.; Bouzidi, L.; Sporns, P. Physical properties of polyurethanes produced from polyols from seed oils. I-elastomers. *J. Am. Oil Chem. Soc.* **2007**, *84*, 55–63.
- (17) Narine, S. S.; Yue, J.; Kong, X. Production of polyols from canola oil and their chemical identification and physical properties. *J. Am. Oil Chem. Soc.* **2007**, *84*, 173–179.
- (18) Neff, W. E.; Mounts, T. L.; Rinsch, W. M.; Konishi, H.; Elagaimy, M. A. Oxidative stability of purified canola oil triacylglycerols with altered fatty-acid compositions as affected by triacylglycerol composition and structure. *J. Am. Oil Chem. Soc.* **1994**, *71* (10), 1101–1109.
- (19) Elfman-Borjesson, I.; Harrod, M. Analysis of non-polar lipids by HPLC on a diol column. *J. High Resolut. Chromatogr.* **1997**, *20* (9), 516–518.
- (20) Bailey, P. S. The Reactions of Ozone with Organic Compounds. *Chem. Rev.* **1958**, *58* (5), 925–1010.
- (21) Flory, P. J. *Principles of Polymer Chemistry*; Cornell University Press: Ithaca, NY, 1953.
- (22) James, H. M.; Guth, E. Theory of the increase in rigidity of rubber during cure. *J. Chem. Phys.* **1947**, *15* (9), 669–683.
- (23) Painter, P. C.; Shenoy, S. L. A simple-model for the swelling of polymer networks. *J. Chem. Phys.* **1993**, *99* (2), 1409–1418.
- (24) Ferry, J. D. *Viscoelastic Properties of Polymers*, 3rd ed.; Wiley: New York, 1980; Chapter 11.
- (25) Dusek, K.; Duskova-Smrckova, M.; Fedderly, J. J.; Lee, G. F.; Lee, J. D.; Hartmann, B. Polyurethane networks with controlled architecture of dangling chains. *Macromol. Chem. Phys.* **2002**, *203* (13), 1936–1948.
- (26) Dusek, K.; Duskova-Smrckova, M. Polymer networks from precursors of defined architecture. Activation of preexisting branch points. *Macromolecules* **2003**, *36* (8), 2915–2925.
- (27) Czech, P.; Okrasa, L.; Boiteux, G.; Mechin, F.; Ulanski, J. Polyurethane networks based on hyperbranched polyesters: Synthesis and molecular relaxations. *J. Non-Cryst. Solids* **2005**, *351* (33–36), 2735–2741.
- (28) Nielsen, L. E.; Landel, R. F. *Mechanical properties of polymers and composites*, 2nd ed.; Marcel Dekker: New York, 1994; Chapter 4.
- (29) Son, T. W.; Lee, D. W.; Lim, S. K. Thermal and phase behavior of polyurethane based on chain extender, 2,2-bis-[4-(2-hydroxyethoxy)-phenyl]propane. *Polym. J.* **1999**, *31* (7), 563–568.
- (30) Ishida, H.; Allen, D. J. Mechanical characterization of copolymers based on benzoxazine and epoxy. *Polymer* **1996**, *37* (20), 4487–4495.
- (31) Thomas, T. J.; Krishnamurthy, V. N.; Nandi, U. S. Thermogravimetric and mass-spectrometric study of the thermal-decomposition of pbct resins. *J. Appl. Polym. Sci.* **1979**, *24* (8), 1797–1808.
- (32) Javni, I.; Petrovic, Z. S.; Guo, A.; Fuller, R. Thermal stability of polyurethanes based on vegetable oils. *J. Appl. Polym. Sci.* **2000**, *77* (8), 1723–1734.
- (33) Cooney, J. D.; Day, M.; Wiles, D. M. Thermal-degradation of poly-(ethylene-terephthalate)-a kinetic-analysis of thermogravimetric data. *J. Appl. Polym. Sci.* **1983**, *28* (9), 2887–2902.
- (34) Kissinger, H. E. Reaction kinetics in differential thermal analysis. *Anal. Chem.* **1957**, *29* (11), 1702–1706.
- (35) Darwent, B. D. *Bond dissociation energies in simple molecules*; National Bureau of Standards: Washington, DC, 1970.
- (36) Young, R. J.; Lovell, P. A. *Introduction to polymers*, 2nd ed.; Chapman and Hall: New York, 1991; Chapter 5.

BM070016I